

# UC Berkeley

## UC Berkeley Previously Published Works

### Title

Fluorescent biological aerosol particles: Concentrations, emissions, and exposures in a northern California residence

### Permalink

<https://escholarship.org/uc/item/5f849501>

### Journal

Indoor Air, 28(4)

### ISSN

0905-6947

### Authors

Tian, Y  
Liu, Y  
Misztal, PK  
[et al.](#)

### Publication Date

2018-07-01

### DOI

10.1111/ina.12461

Peer reviewed

DR. YILIN TIAN (Orcid ID : 0000-0001-5905-4976)

DR. YINGJUN LIU (Orcid ID : 0000-0001-6659-3660)

PROF. WILLIAM W NAZAROFF (Orcid ID : 0000-0001-5645-3357)

Article type : Original Article

## **Fluorescent biological aerosol particles: Concentrations, emissions, and exposures in a northern California residence**

Yilin Tian<sup>1\*</sup>, Yingjun Liu<sup>2</sup>, Pawel K. Misztal<sup>2</sup>, Jianyin Xiong<sup>3</sup>, Caleb M. Arata<sup>4</sup>,  
Allen H. Goldstein<sup>1,2</sup>, William W Nazaroff<sup>1</sup>

**For submission to:**

*Indoor Air*

<sup>1</sup>Department of Civil and Environmental Engineering, University of California,  
Berkeley, CA 94720, USA

<sup>2</sup>Department of Environmental Science, Policy, and Management, University of  
California, Berkeley, CA 94720, USA

<sup>3</sup>School of Mechanical Engineering, Beijing Institute of Technology, Beijing  
100081, China

<sup>4</sup>Department of Chemistry, University of California, Berkeley, CA 94720, USA

This article has been accepted for publication and undergone full peer review but has not been through the copyediting, typesetting, pagination and proofreading process, which may lead to differences between this version and the Version of Record. Please cite this article as doi:

10.1111/ina.12461

This article is protected by copyright. All rights reserved.

\*Corresponding author. E-mail:tiany@berkeley.edu

## **Keywords**

Bioaerosols; Built environment; Human activity; FBAP; Occupancy; Sources

## **Abstract**

Residences represent an important site for bioaerosol exposure. We studied bioaerosol concentrations, emissions, and exposures in a single-family residence in northern California with two occupants using real-time instrumentation during two monitoring campaigns (eight weeks during August-October 2016 and five weeks during January-March 2017). Time- and size-resolved fluorescent biological aerosol particles (FBAP) and total airborne particles were measured in real time in the kitchen using an ultraviolet aerodynamic particle sizer (UVAPS). Time resolved occupancy status, household activity data, air-change rates, and spatial distribution of size-resolved particles were also determined throughout the house. Occupant activities strongly influenced indoor FBAP levels. Indoor FBAP concentrations were an order of magnitude higher when the house was occupied than when the house was vacant. Applying an integral material balance approach, geometric mean total FBAP emissions from human activities observed to perturb indoor levels were in the range of 10-50 million particles per event. During the summer and winter campaigns, occupants spent an average of 10 and 8.5 hours per day, respectively, awake and at home. During these hours, the geometric mean daily-averaged FBAP exposure concentration (1-10 micrometer diameter) was similar for each subject at 40 particles/L for summer and 29 particles/L for winter.

## **Practical Implications**

Developing knowledge about bioaerosol sources and dynamic behavior in residences can contribute to a better understanding of human exposures. Human occupancy played an essential role influencing FBAP levels in a single-family residence. Measured emission factors for common FBAP source activities can be used in indoor air quality models.

## 1 Introduction

Bioaerosols are airborne biological particles and can include viruses, bacteria, fungi, pollen, and their fragments, among other materials. Bioaerosols are omnipresent in outdoor and indoor air. They can occur as independent entities or in the form of aggregated cells or spores, as fragmented biological materials, and as materials of biological origin attached to abiotic particulate matter.<sup>1</sup> Some indoor bioaerosol particles are in the respirable size range. For instance, Yang et al.<sup>2</sup> reported that airborne influenza viruses measured indoors were mainly associated with fine particles ( $< 2.5 \mu\text{m}$ ). In an occupied classroom, human-associated bacteria were primarily detected on particles in the diameter range  $3\text{-}5 \mu\text{m}$ .<sup>3</sup> Several studies have reported that unicellular fungal spores found indoors are in the range  $2\text{-}5 \mu\text{m}$  in aerodynamic diameter.<sup>4-7</sup>

Non-occupational exposure to indoor bioaerosols has been associated with several detrimental health outcomes, such as infectious disease transmission (i.e., influenza, tuberculosis, Legionnaires' disease), and allergic asthma and rhinitis.<sup>8-9</sup> Bioaerosol concentrations and composition vary among built environments, such as public facilities, offices, and dwellings, with the differences attributable, at least in part, to different occupancy levels and building characteristics.<sup>10-12</sup>

Residential environments are of particular interest as a site of bioaerosol exposure because of the large proportion of time that people spend in their homes. For example, the NHAPS study showed that people in the United States on average spent 70% of their time indoors at home.<sup>13</sup> Good knowledge of the sources and dynamic behavior of bioaerosols in residential environments is therefore essential for characterizing overall exposures to bioaerosols.

Indoor bioaerosol levels are governed by a balance among several factors, the primary ones being emissions from indoor sources, intrusion from outdoor air, and removal from indoor

air by a combination of filtration, deposition, and ventilation. Previous studies demonstrated that human occupancy can be an important source of indoor bioaerosols.<sup>14-17</sup> Human occupants can influence airborne biological particle levels in residences via respiratory emissions (i.e. sneezing), shedding of bacteria-laden skin flakes, movement-induced resuspension from clothing, upholstery materials, mattress, and flooring, and other ordinary household activities, such as showering, handling fabrics, sweeping floors and vacuuming.<sup>14,16,18-23</sup> Activities such as these result in strong enhancements of bioaerosol concentrations, often over short periods. Considering the potential for rapidly changing indoor bioaerosol concentrations, sampling methods with high time resolution can make important contributions to the state of knowledge regarding bioaerosol exposures in residential environments. Real-time measurements also can be used for estimating source-specific emission rates. Previous studies assessing bioaerosol concentrations in dwellings have mostly relied on time-integrated sampling (several hours or longer) or snapshots samples (no longer than several minutes).<sup>6,10,16,12,17,24</sup> To our knowledge, there are no reported studies of residential bioaerosol concentrations that incorporate continuous, high time-resolution monitoring over extended periods. Moreover, bioaerosol emissions caused by household activities have not been well-characterized.

To contribute toward filling these important knowledge gaps, the primary goal of this work was to investigate time- and size-resolved levels of bioaerosol concentrations in a residential environment. In particular, the effect of human occupancy and activities on indoor bioaerosol concentrations was evaluated. Bioaerosol concentrations were monitored in a single-family home throughout two multiweek observational campaigns using an ultraviolet aerodynamic particle sizer (UVAPS). Following previous practice,<sup>25</sup> we will refer to the fluorescent particles measured by the UVAPS (particle size: 1-10  $\mu\text{m}$ ) as fluorescent biological

aerosol particles (FBAPs), which are considered to be a lower bound estimate of primary biological aerosol particles. Occupancy status and household activity data were acquired using occupant-maintained logs plus supplementary electronic sensors. Additional monitoring information was obtained to provide air-change rate data and also the spatial distribution of size-resolved particles (without regard to fluorescence) throughout the house. A second objective is to report on human activity-induced FBAP emissions as a function of particle size and activity type. For this purpose, an integral material balance was applied to the measured FBAP concentrations to quantify emissions per event. Emissions were characterized based on observational data for various cooking activities and for vacuuming. Emissions were also characterized for a few controlled experiments conducted in the same residence by researchers. A third goal of the study is to characterize exposures of the household occupants. To our knowledge, this study is the first to report FBAP concentrations, emissions and exposures in a residence under normally occupied conditions.

## **2 Methods**

### **2.1 Site description**

Bioaerosol concentrations were monitored in a single-family split-level home with a total floor area of 170 m<sup>2</sup> and two adult residents (female designated F1 and male M1) in Oakland, California. The selected house was built in 1938. The volume of the house's normally occupied space is about 350 m<sup>3</sup>, considering ordinarily occupied rooms, including bathrooms, and subtracting the estimated volume of cabinetry, furniture, and closets. There is hard flooring throughout. A floor plan of the house is presented in Figure S1. The lower level consists of a kitchen, family room, and living room. The kitchen, which is equipped with an electric stove, range hood and appliances, also has a small dining area. The family room, which is also the TV

room, is connected through an open doorway to the kitchen/dining area. The living room, which is infrequently used, faces the family room on the opposite side of the entrance hallway/foyer.

The upper level, reached via six stairs, contains the master bedroom, two guest bedrooms and two bathrooms, with a small landing space connecting the top of the stairs to all of the bedrooms.

The doors between the rooms on the lower level and the bedroom doors to the landing were consistently left open during monitoring. Area rugs cover most of the hardwood floors in the family room, living room and guest bedrooms. The master bedroom, landing, and hallway have hardwood flooring and the kitchen/dining area has vinyl-type flooring. There is no visible water damage in the living spaces, no household pets, and no indoor plants other than several orchids in the family room. The back yard of the property contains a fruit and vegetable garden plus a detached garage.

Multiweek contiguous observational monitoring campaigns were conducted during summer 2016 (eight weeks of bioaerosol monitoring, beginning in mid-August) and winter 2017 (five weeks, beginning in late January), with supplementary experiments carried out at the end of the summer campaign. The summer campaign coincided with the dry season of northern California. The average  $\pm$  standard deviation of the indoor temperature during summer was  $22.4 \pm 1.6$  °C and the corresponding relative humidity was  $65 \pm 6\%$ . During the winter campaign, it rained frequently. The indoor temperature was  $17.6 \pm 1.3$  °C and the relative humidity was  $71 \pm 4\%$ . The house has no mechanical ventilation other than exhaust fans above the stove and in the bathrooms; otherwise, the house is ventilated through a combination of infiltration and natural ventilation through operable windows. There is no air conditioning. There was sporadic use of central heating during the winter campaign. Determined using continuous controlled tracer releases (inert, isotopically labeled tracers were used: propene-d6, propene-d3, and butene-d3),

the geometric mean air change rate (geometric standard deviation) was  $0.47 \text{ h}^{-1}$  (1.6) for the summer campaign and  $0.33 \text{ h}^{-1}$  (1.3) for the winter campaign.<sup>26</sup> The higher value in the summer is attributed to window opening being more common during that season.

## 2.2 Sampling protocols

During the observational campaigns, the two occupants were encouraged to follow their normal daily routines. They maintained daily logs of the times of their presence (separately recording awake and asleep times) and absence from the home. They also maintained a daily log of basic household activities, such as cooking and cleaning. The occupants gave informed consent for this study, which was approved by the Committee for Protection of Human Subjects at the University of California, Berkeley (Protocol #: 2016-04-8656). Fluorescent biological aerosol particle concentrations were only monitored locally in the kitchen/dining area of the house, because of the challenge in effectively transmitting particles as large as  $10 \mu\text{m}$  through long sampling lines. The kitchen is the most frequently used room on the lower level. Besides cooking and eating, normal desk work (i.e., working with a laptop) often occurs at the dining table. Owing to the instrument location, we focused on assessing emissions and exposures during the times that the occupants were awake and at home. The data collected during the observational campaigns were judged unsuitable to assess FBAP exposures during sleep.

Using optical particle counters, size- and time-resolved particle levels were monitored without regard to fluorescence in three locations (lower level: family room, kitchen; upper level: landing) to evaluate spatial variability of particle concentrations inside the house; outdoor levels were sampled simultaneously. Also, the total particle number concentration (mainly ultrafine particles, UFP) was measured in the living room, providing supplementary evidence about the timing of source activities such as cooking and vacuuming. Wireless sensors were installed in



each room to monitor environmental conditions, occupancy, appliance usage, and window/door state (open vs closed). In addition, volatile organic compounds, ozone, carbon dioxide and inert tracer gas concentrations were monitored in real time, as reported in detail in Liu et al.<sup>26</sup> The field campaign team visited the house on a weekly basis for instrument maintenance and data collection. At the end of each campaign, outdoor FBAP levels were monitored on site for about two days.

### **2.3 Manipulation experiments**

Supplementary manipulation experiments were conducted at the end of the summer campaign to probe FBAP emissions associated with common activities that occurred on the upper level. A researcher (female) conducted scripted activities, including showering, making the bed and folding clothes, and vacuuming in the master bedroom and bathroom. Details about these experiments are reported in the Supporting Information.

During the manipulation experiments, dark colored clothing, blanket, and bedding were used to minimize any interference of non-biological fluorescent material, such as optical brightening agents used on white fabrics. The master bedroom door and windows were closed so that the space could be considered as an enclosed single compartment. The master bathroom door, which is connected to the master bedroom, remained open during the manipulation experiments. FBAP levels were measured directly in the master bedroom. Air-change rates for the isolated bedroom/bathroom zone were determined using decay periods of metabolically generated carbon dioxide. The house occupants were away from home during these experiments.

### **2.4 Instrumentation**

An ultraviolet aerodynamic particle sizer (UVAPS; model 3314; TSI Inc, Shoreview, MN, USA), which provides time-resolved single particle detection of size-resolved viable biological

particles using laser-induced fluorescence (LIF), was used in the study. The UVAPS uses a fixed excitation wavelength of 355 nm which is produced by a diode pumped, solid-state laser, and an emission region of 420 to 575 nm. Autofluorescence under this condition is associated with biochemical fluorophores, such as metabolic function riboflavin and reduced pyridine nucleotides coenzymes (e.g. NAD(P)H), which are active cellular metabolism fingerprints.<sup>27-29</sup> In prior studies, the UVAPS has been utilized to measure outdoor<sup>25,30-33</sup> and indoor bioaerosols, such as bacteria and fungal spores.<sup>14,15,34</sup> Studies have shown that potential abiotic fluorescent interferents, such as humic-like substances, polycyclic aromatic hydrocarbons (PAH), certain secondary organic aerosols (SOA), soot, and mineral dust can contribute to false-positive counts.<sup>35-37</sup> For outdoor conditions, the interference of abiotic materials was found to be weak for particles larger than 1  $\mu\text{m}$ .<sup>25,37</sup> We adopt the practice of focusing attention on particles larger than 1  $\mu\text{m}$  to exclude potentially strong contributions from known interferents. For residential environments, some extra concerns arise because of the potential for sources such as cooking emissions, optical brightening agents, and fabric fibers shed or resuspended from clothing, carpet, and upholstery to contribute to the fluorescence signal.<sup>38</sup>

The UVAPS reports aerodynamic diameter, concentration, and the fluorescence intensity of particles for diameters in the range 0.5 to 15  $\mu\text{m}$ ; there are 52 size channels and 64 fluorescent intensity channels. Particles measured by the UVAPS were sorted into three groups based on their fluorescent intensity (FI, reported without units): total particles,  $N_T$  (FI  $\geq 0$ ); fluorescent biological aerosol particle (FBAP),  $N_F$  (FI  $\geq 2$ ); and highly fluorescent particles,  $N_{F20}$  (FI  $\geq 20$ ). In assessing the fluorescent particles, we excluded fluorescence intensity channel 2 (FI = 1) to avoid interference from non-fluorescent particles.<sup>25,39</sup> In a study in an occupied classroom, Bhangar et al.<sup>14</sup> found that indoor FBAP exhibited a characteristically bimodal FI distribution;

that study included a report of the highly fluorescent portion of FBAP. This study adopted that same concept and used the same threshold as in Bhangar et al.<sup>14</sup> In addition to clustering by fluorescence intensity, for some of the data analysis, the particle sizes were clustered. In particular, for FBAP, the UVAPS particle size channels in the 1-10 micron aerodynamic diameter range were combined into 3 bins: 1-2.5 micron, 2.5-5 micron, and 5-10 micron. In this study, fluorescent biological aerosol particles that are smaller than 1  $\mu\text{m}$  or larger than 10  $\mu\text{m}$  were excluded due to known interference and big spatial variability caused by rapid deposition, respectively. The UVAPS sampled air at a flow rate of 1 L/min (plus 4 L/min for sheath air), and recorded data with 1-minute time resolution. With the sample flow rate and chosen resolution, the minimum detection limit was 1.2 particles/L. The UVAPS was placed in a soundproof box, equipped with cooling fans, and situated next to the dining table in the kitchen. A 0.3-m length of electrically conductive tubing was employed to sample air at 1.2 m in height, which corresponds to the breathing zone of a seated person. At the end of each campaign, separate from the manipulation experiments, the UVAPS was moved to the upper level to sample outdoor air through a window panel with a 0.6-m length of conductive tubing. The UVAPS sampling efficiency was evaluated for both conditions, as reported in Figure S2. The UVAPS response was adjusted to correct for sampling losses for the outdoor measurements. Particle loss in the tubing for indoor measurements was judged small enough to neglect.

Four optical particle counters (OPC; model MET ONE HHPC 6+; Beckman Coulter, Brea, CA, USA) were used to measure particle concentrations indoors and outdoors in the diameter range 0.3 to 10  $\mu\text{m}$  in 6 size channels at a sample flow rate of 2.83 L/min. After manufacturer calibration, the four OPCs were initially deployed in the middle of the summer campaign. For the winter campaign, the OPCs were deployed together with UVAPS throughout.

A water-based condensation particle counter (WCPC, model 1120; MSP Corp., Shoreview, MN, USA) was utilized to measure total number concentration of particles down to 8 nm at a sample flow rate of 1 L/min. All particle instruments were set to record measurement results with 1-minute resolution.

Wireless indoor climate monitors (Netatmo, Boulogne-Billancourt, France) were deployed to measure temperature, relative humidity, and carbon dioxide concentration.

Additional wireless sensors (SmartThings, Inc., Mountain View, CA, USA) were used to monitor room occupancy (motion sensors), window and door open/closed status (multipurpose sensors), appliance usage (smart outlets and multipurpose sensors), and basic environmental conditions (temperature and relative humidity sensors). Appliances monitored for operational status were the dishwasher, electric convection oven, microwave oven, coffee maker, toaster, washer and dryer. During the winter campaign, a temperature sensor was placed above one of the heater supply registers as an indicator of when the furnace operated.

## **2.5 Quality assurance**

Instrument maintenance and zero count checks were carried out throughout the observational campaigns. Instrument flow rates were confirmed by use of a primary standard flow meter (model: Defender 510; Mesa Laboratories, Butler, NJ, USA). Before and after each campaign, UVAPS sizing and fluorescence response were checked using monodispersed polystyrene latex (PSL) particles and fluorescent particles spanning the size range 0.6 to 4.8  $\mu\text{m}$  (Duke Scientific Corp., Fremont, CA, USA; Thermo Scientific, Fremont, CA, USA). The UVAPS performance was found to agree well with the manufacturer's set values, as shown in Figure S3. The manufacturer calibrated the OPCs prior to the summer campaign. The OPC readings were adjusted using the ratio of measured actual flow rate to target flow rate (2.83

L/min). Collocation tests were completed pre- and post-campaign in the laboratory; the resulting adjustment factors (AF) are presented in Table S8. One OPC was designated to be the reference unit. For each campaign, the average AFs of pre- and post-campaign tests was used to adjust the readings of the other OPCs to the reference unit. After adjustment, differences between OPC responses were less than 10%.

## **2.6 Data analysis**

In assessing indoor concentrations and exposures, certain periods were excluded because of missing data or because of nonrepresentative conditions. Specific exclusion periods, detailed in the SI, were times when the research team was in the house (e.g. for calibration and instrument servicing), periods of instrument malfunctioning, and periods when occupants deliberately left the home vacant for research purposes. We did not evaluate directly the contributions of outdoor air to indoor FBAP levels owing to the lack of simultaneous indoor and outdoor FBAP measurement. However, available evidence, detailed subsequently, suggests that outdoor contributions represented a small proportion of the total indoor FBAP levels, especially when the occupants were awake and at home.

### **2.6.1 Effect of occupancy**

Activity patterns of the two occupants, F1 and M1, were obtained from occupant-maintained presence-absence logs. Specifically, occupants recorded each day the times that they were (a) at home asleep (including evening and morning hours in bed); (b) at home, indoors, and awake; (c) at home but outdoors; and (d) away from home. These times were recorded with an approximate resolution of 5 minutes. Household occupancy, defined as the proportion of time that the house was occupied (by either one or both occupants), was estimated based on occupant activity pattern logs.

To study the effect of occupancy on indoor FBAP concentration, UVAPS data were sorted into three groups based on occupancy level: home vacant, one occupant at home awake, and two occupants at home awake. Home vacant condition included the periods when both occupants were away from home during normal days and the periods when the house was left vacant deliberately for research purposes. Hourly average FBAP concentrations for each occupancy condition were estimated using the following criteria. For a given hour, if occupancy level remained the same for more than 45 minutes, then the arithmetic mean of the UVAPS data collected under this occupancy level was used as the average concentration for that hour. If no single occupancy condition was maintained for at least 45 minutes, then the UVAPS data collected during that hour were excluded from this assessment. Additional time-filters were applied to discern appropriate home-vacant conditions. For each home-vacant interval, data collected from the first three vacant hours were excluded to avoid interference from the persistence of a signal that originated from emissions occurring when the house was last occupied. In addition, data collected overnight (11 pm to 6 am) were systematically excluded in this analysis because the purpose was to examine the influence of occupancy during awake hours.

### **2.6.2 Emission estimation**

Some occupant activities (notably cooking) produced discernible increases in FBAP concentrations. We used a material-balance model to estimate FBAP emissions from the concentration increases caused by such activities as recorded during the observational campaigns. Activities were selected based on the following criteria: 1) activity start time could be clearly identified, and 2) activity is expected to have the potential to emit FBAP. Four types of activities met these conditions: breakfast preparation (daily; both campaigns), other cooking (e.g., dinner preparation; almost daily; both campaigns), making applesauce (about 3 times per week; summer

campaign only), and vacuuming (biweekly; both campaigns). For each activity, the start time and the activity duration,  $t_s$ , were obtained from occupant-maintained activity logs. When the  $t_s$  value was not available from the activity logs, event duration,  $T$ , was specified to be a time that was believed to be longer than  $t_s$ . In selecting values of  $T$  for each activity, we considered input information from measured FBAP concentration time series, co-pollutant data (i.e. ultrafine particle concentration) and wireless sensor information. A detailed description can be found in the SI. The geometric mean (geometric standard deviation) event durations were 51 (1.4) minutes, 31 (1.5) minutes, 90 (1.2) minutes, and 25 (1.3) minutes for breakfast preparation, other cooking, making applesauce, and vacuuming, respectively.

We quantified emissions to determine the total number of FBAP particles released during an event,  $F$ . As compared to assessing average emission rates (e.g., number of FBAP particles emitted per hour), this approach has the benefit of being insensitive to the accurate determination of event duration. Total FBAP particle emissions per event was estimated by solving a single-compartment material-balance model, as shown in equation 1. This equation states that for the  $j^{\text{th}}$  particle size interval, the change rate of indoor FBAP concentration  $N_{F,in,j}$  (particles/m<sup>3</sup>) can be obtained by summing contributions from indoor sources ( $E(t)$ , particles per hour) plus infiltrated outdoor particles minus the removal of indoor particles by means of ventilation and deposition. In equation 1,  $V$  is the mixing volume of the interior space in which the emissions occurred (m<sup>3</sup>),  $a$  is air change rate (h<sup>-1</sup>),  $p$  is the particle penetration efficiency (-),  $N_{F,out,j}$  (particles/m<sup>3</sup>) is outdoor FBAP concentration, and  $k$  is particle deposition rate coefficient (h<sup>-1</sup>).

$$\frac{dN_{F,in,j}(t)}{dt} = \frac{E(t)}{V} + apN_{F,out,j} - (a + k)N_{F,in,j}(t) \quad (1)$$

Equation 2 is obtained by multiplying each side of equation 1 by  $V$  and then integrating over the period from source start time ( $t = 0$ ) to the end of event duration ( $t = T$ ).

$$V \int_0^T d(N_{F,in,j}) = \int_0^T E(t)dt + apV \int_0^T N_{F,out,j}(t)dt - (a+k)V \int_0^T N_{F,in,j}(t)dt \quad (2)$$

To proceed, we assume that the identified activity is the only emission source of FBAP within the time of the event,  $0 \leq t \leq T$ . The total number of FBAP emitted,  $F$ , is obtained as the integral of  $E$  over time, as shown in equation 3.

$$F_j = \int_0^T E(t)dt \quad (3)$$

The evaluation of FBAP emissions is thus obtained by substituting equation 3 into equation 2, and rearranging to yield equation 4:

$$F_j = V \left[ N_{F,in,j}(T) - N_{F,in,j}(0) + (a+k)T \overline{N_{F,in,j}(T)} - apT \overline{N_{F,out,j}} \right] \quad (4)$$

In application,  $N_{F,in,j}(0)$  is assessed as the 5-min average indoor FBAP concentration immediately before time  $t = 0$ , and  $N_{F,in,j}(T)$  is the 5-min average centered at time  $T$ . For the observational campaigns, the volume of the house living space,  $350 \text{ m}^3$ , was used as the mixing volume  $V$ . Using this volume raises a risk of bias in the analysis attributable to nonuniform concentrations in the household. In particular, the approach may overestimate the emissions for source activities in the kitchen to the extent that the measured FBAP concentrations in the kitchen exceed the household indoor average. To minimize any error associated with nonuniform concentrations, we applied a scaling factor,  $s$  (-) to estimate house-average FBAP concentrations based on those measured in the kitchen, as shown in equation 5.

$$F_j = V \left[ s_j(T)N_{F,in,j}(T) - s_j(0)N_{F,in,j}(0) + s_j(T)(a+k)T \overline{N_{F,in,j}(T)} - apT \overline{N_{F,out,j}} \right] \quad (5)$$



Total particle data obtained from the three OPCs (placed, respectively, in the kitchen, family room, and landing) were used to estimate  $s$ , which is defined as the ratio of house-volume-weighted average particle concentration to kitchen particle concentration. For this purpose, the living spaces were grouped into three sections corresponding to the OPC locations: kitchen plus adjacent hallway, the rest of lower level area, and the upper level. According to the volume of each section, the weighting factors assigned to the kitchen, family room and landing OPCs were 0.2, 0.4, and 0.4, respectively. Corresponding to the OPC size channels, the UVAPS data were grouped in three size bins: 1-2  $\mu\text{m}$ , 2-5  $\mu\text{m}$ , and 5-10  $\mu\text{m}$ . Note that the first size cut is different from that used in exposure assessment. In this analysis, the spatial variability of the  $N_F$  to  $N_T$  ratio, and differences in aerodynamic diameter (as measured by the UVAPS) and optical diameter (as measured by the OPCs) attributable to particle shape and density were assumed to be negligible. Scaling factors,  $s$ , used for the four types of source activities are summarized in Table S9. The OPC data reveal that air was relatively well-mixed throughout the house for the food-related emission events (breakfast, cooking, and applesauce making). The scaling factor adjustments required mostly less than 20% correction to determine household average concentrations based on measured values in the kitchen.

Real-time air-change rates with 2-h resolution were determined, as reported in Liu et al.,<sup>26</sup> using constantly released and continuously monitored tracer-gas concentrations. Data collected in this study were not sufficient to determine a size-resolved particle penetration factor,  $p$ . Hence,  $p$  was assumed to be 1 (-) for all particle size bins of interest, resulting in an upper bound estimate of the contribution to indoor levels from outdoor air,  $apT\overline{N_{F,\text{out}}}$ . As presented in Table S7, the mean outdoor FBAP concentration measured at the end of each campaign was used as  $\overline{N_{F,\text{out}}}$  for estimating emission factors for events taking place in the corresponding campaign.

Size-resolved particle decay rate coefficients,  $k$ , were determined using data from Thatcher et al.<sup>40</sup> For the particle size bins 1-2  $\mu\text{m}$ , 2-5  $\mu\text{m}$ , and 5-10  $\mu\text{m}$ ,  $k$  values used in this study were 0.37  $\text{h}^{-1}$ , 2.3  $\text{h}^{-1}$  and 7.2  $\text{h}^{-1}$ , respectively.

FBAP concentrations measured during the hour prior to each episodic source event were examined to ascertain whether previous source events were still evident, as indicated by concentrations persistently and substantially elevated above baseline and decaying from the previous event. When applicable, the contribution of a previous source was modeled by performing a curve fit to the decay trend. The value of  $N_{\text{F},\text{in}}$  used in equation 5 was the measured indoor FBAP concentration minus the modeled contribution from any previous source event.

For the manipulation experiments, the same approach applied in the observational campaign was used to determine values for  $\overline{N_{\text{F},\text{out}}}$ ,  $p$  and  $k$ . The mixing volume for the manipulation experiments,  $V$ , was 47  $\text{m}^3$ , determined as the volume of the master bedroom plus master bathroom. In these manipulation experiments, scaling factors are not needed, so equation 4 was used to calculate total emissions,  $F$ . The source duration,  $t_s$ , for each type of scripted activity is reported in Table S1. Air-change rates for the master bedroom were determined during the manipulation experiments using the decay period of metabolically generated carbon dioxide, measured with the room vacant after completing the simulated activity.

### 2.6.3 Exposure assessment

The quantification of FBAP exposure at home was assessed on a daily-integrated basis for each of the household occupants. For each calendar day monitored and for each occupant considered separately, this measure reflects the time-integral of the FBAP concentration during the periods that the occupant was awake and at home. It is expressed in units of number of fluorescent particles per cubic meter multiplied by awake hours per day ( $\text{particles}/\text{m}^3 \times \text{h}/\text{d}$ ).

This measure can also be expressed as the average daily FBAP exposure concentration during the period of awake occupancy multiplied by the hours per day spent awake at home, as illustrated in Fig. S4. The FBAP concentration measured in the kitchen was deemed suitable to be used as the measure of FBAP exposure concentration during awake times because the kitchen was the most commonly used room during the day. We specifically excluded any contribution to FBAP exposure during sleep because data collected in the kitchen does not adequately represent the concentration in the master bedroom, especially in the breathing zone, and especially for coarse particles (2.5-10  $\mu\text{m}$ ).

#### **2.6.4 Statistical analysis**

Statistical analysis was conducted using Minitab® 16 Statistical Software (Minitab Inc., State College, PA). For each set of data, Anderson-Darling normality test was performed first to evaluate if the data fit a normal distribution. Parametric statistics, such as Student's t-test, were used for data sets which passed the normality test with confidence level of 95% ( $\alpha = 0.05$ ). For those failed the normality test, non-parametric statistics were used, such as Mann-Whitney U test ( $\alpha = 0.05$ ).

### **3 Results and Discussion**

#### **3.1 Indoor FBAP levels and the influence of occupancy**

Figure 1 illustrates the diurnal trends of indoor FBAP number concentrations measured in the kitchen for the summer (Figure 1a) and winter campaign (Figure 1b), together with house occupancy patterns. Analysis for the summer campaign spanned 34 days, from Aug 20<sup>th</sup> to Sep 24<sup>th</sup>, 2016, and for the winter campaign 23 days from Jan 31<sup>st</sup> to Feb 28<sup>th</sup>, 2017. In total, occupants spent about 45% (F1 = 45%, M1 = 44%) and 38% (F1 = 37%, M1 = 39%) of their

total time awake and at home during the summer and winter campaign periods, respectively.

More detailed information about the occupancy patterns is reported in the SI (Figure S5 and S6).

As is clearly evident in Figure 1, indoor FBAP concentrations correlated strongly with household occupancy. Concentrations were low and remained steady when occupants were asleep; elevated concentrations were observed in all three indicators —  $N_F/N_T$ ,  $N_F$ , and  $N_{F20}$  — when the occupants were awake and at home. Chen and Hildemann have reported an analogous observation of enhanced residential bioaerosol concentrations during daytime hours.<sup>16</sup>

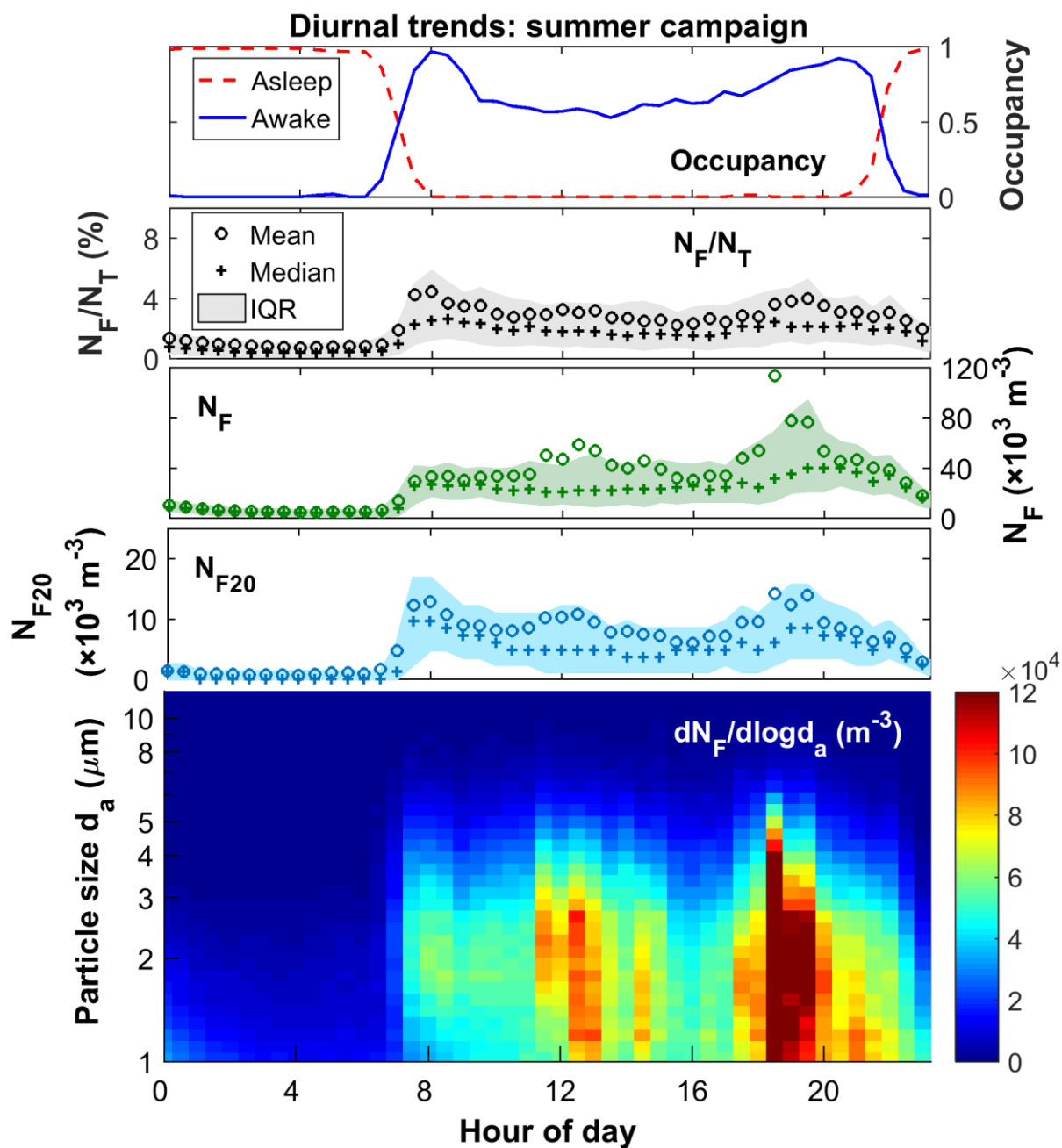
For both summer and winter campaigns, the diurnal patterns of  $N_F/N_T$ ,  $N_F$ , and  $N_{F20}$  exhibited peaks during the morning (7:30-9 am) and evening (5-8:30 pm) hours that correspond with breakfast and dinner meal preparation periods. During these intervals, not only was the average occupancy level higher (as exhibited in the top frames of Figure 1) but the occupants would also have tended to be more frequently in the kitchen and more active than the average during other intervals.

In the diurnal patterns displayed in Figure 1, the morning and evening peaks are remarkably similar. For example, the median  $N_F$ ,  $N_{F20}$ , and  $N_F/N_T$  values of the morning and evening peaks agree to within 10%, except for  $N_F$  during the summer campaign, for which a 30% higher value was observed during evening hours.

The diurnal patterns exhibited many qualitative similarities between seasons, but also some differences. Mean and median values are seen to be similar for the winter campaign, but exhibited some differences during the summer campaign. For example, additional peaks in mean  $N_F$  concentrations, which exceeded the interquartile range, are observed during summer at around noon, even though the occupancy pattern remained steady. Higher mean to median ratios were also observed during evening hours, 6-7 pm. These elements reflect higher variability across

sampling days and particularly reflect positive skewness in the distributions of concentrations measured during these hours. The effects trace back to cooking-related activities, which were more frequent at lunch time during the summer than during the winter and also included more frequent and more intensive episodes in the summer overall. The emissions associated with cooking particularly influenced the mean concentrations of particles in the diameter range 1-5  $\mu\text{m}$ . Similar effects, although less pronounced, are observed for  $N_{F20}$ . This evidence supports an inference that episodic sources had a greater influence on indoor FBAP levels during summer than during winter at this site.

(a)



(b)

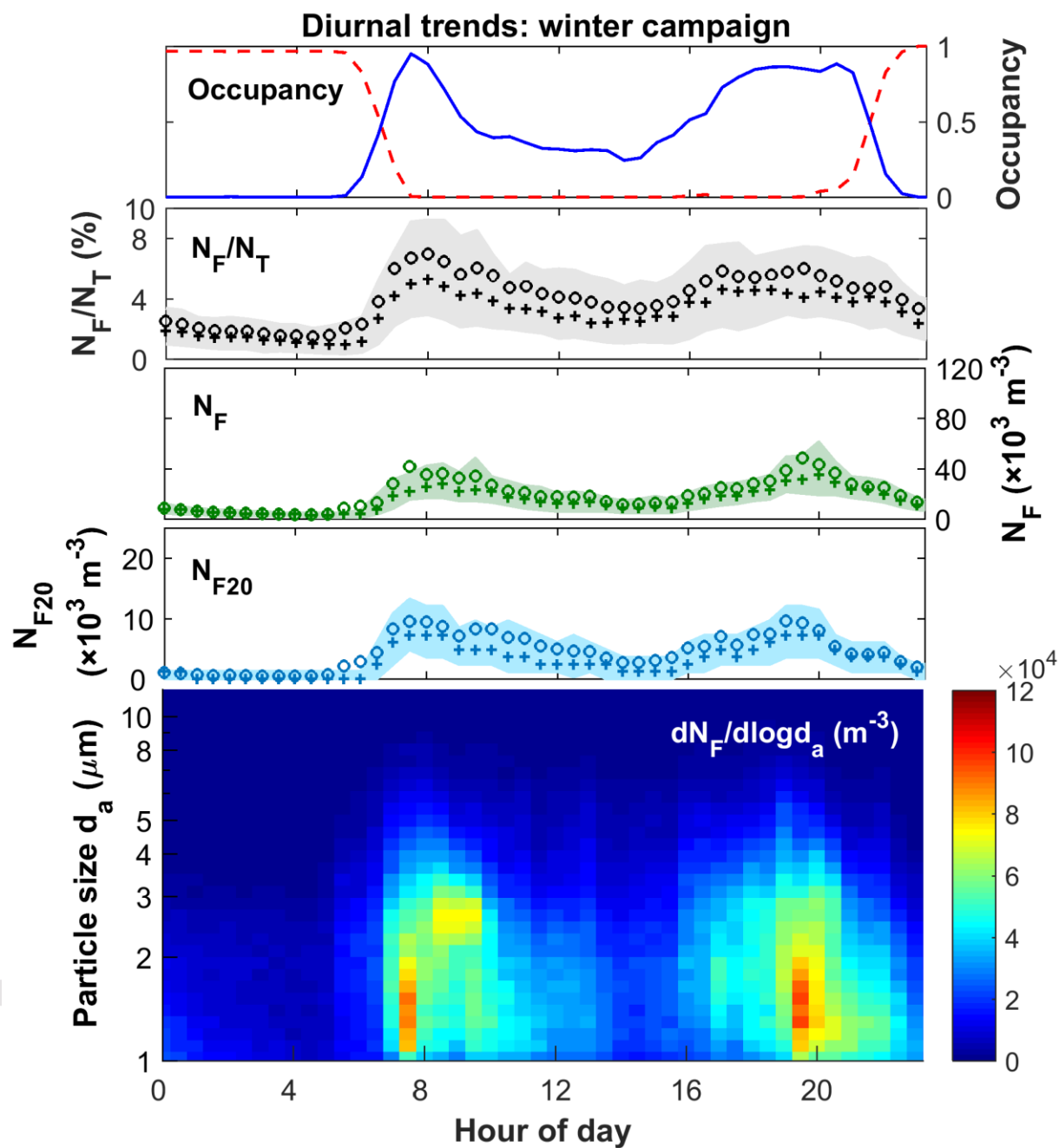


**Figure 1.** Diurnal trends of occupancy and indoor FBAP number concentrations measured in the kitchen for (a) summer and (b) winter campaigns. The top panel presents the proportion of time the house was occupied associated with occupant activity patterns (awake or asleep). The middle three panels show the ratio of fluorescent to total particles ( $N_F/N_T$ ), the size-integrated (1-10  $\mu\text{m}$ ) FBAP concentrations ( $N_F$ ), and the highly fluorescent particle concentrations ( $N_{F20}$ ), respectively. The bottom panel displays the mean FBAP size distributions.

To further explore the influence of human occupancy on indoor FBAP levels, the time series of size-segregated  $N_F$  and  $N_{F20}$  concentrations were grouped into three categories based on occupancy level; Figure 2 displays the corresponding geometric mean (GM) values of hourly averaged concentrations in relation to occupancy state. Compared with house-vacant condition, occupancy was associated with an order of magnitude increase in  $N_F$  and  $N_{F20}$  concentrations. Furthermore, having two occupants in the house was associated with systematically higher FBAP levels than having a single occupant. Significantly higher  $N_F$  and  $N_{F20}$  concentrations and also a higher ratio of fluorescent to total particles ( $N_F/N_T$ ) were observed when two occupants were at home for both monitoring campaigns ( $p < 0.001$ , Mann-Whitney test).

In the evening of one of the summer campaign days, about 20 people were at the house for a dinner party. The hourly average  $N_F$  and  $N_{F20}$  observed during the party hour were  $320 \times 10^3 \text{ m}^{-3}$  and  $73 \times 10^3 \text{ m}^{-3}$ , respectively, close to the 90<sup>th</sup> percentile of  $N_F$  and  $N_{F20}$  concentrations associated with two occupants being awake and at home during the summer campaign. This finding is consistent with results of Bhangar et al.<sup>15</sup> and Heo et al.<sup>41</sup>, who, respectively, reported enhanced FBAP emissions and bacterial bioaerosols associated with increased number of human occupants. Clearly, human occupancy is a prominent source of FBAPs in the monitored residence; the low overnight levels presented in Figure 1 indicate that the human-associated source is more associated with activity than with simple presence.

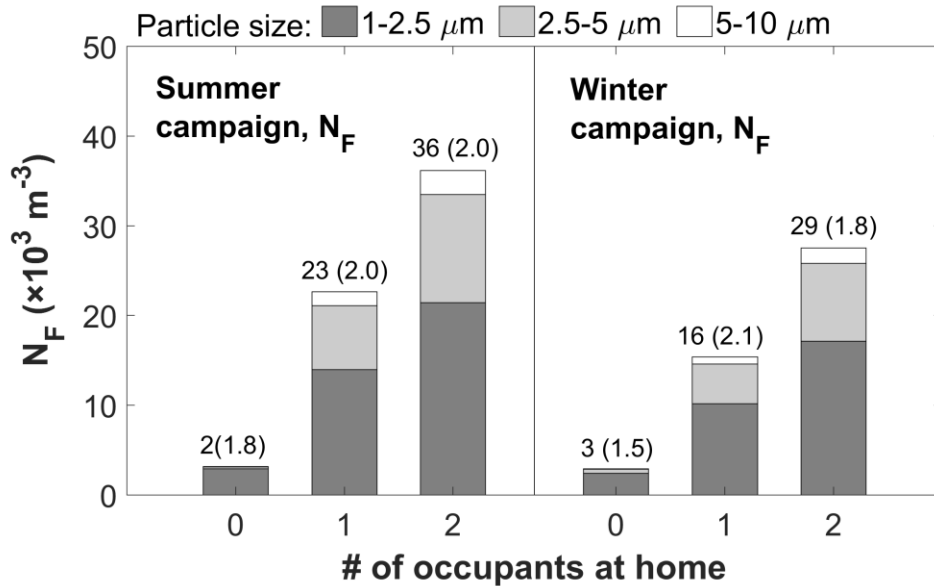
Besides occupancy level, Figure 2 shows a perceptible influence of season on indoor FBAP levels. Statistically significant differences between the summer and winter campaigns were detected for  $N_F$  and  $N_{F20}$  levels associated with occupied conditions (1 and 2 occupants). Levels were higher in summer than in winter ( $p < 0.001$ , one-sided Mann-Whitney test). It is noteworthy that the higher levels occurred in summer despite higher air-change rates during that



season. The enhanced  $N_F$  and  $N_{F20}$  concentrations in the summer are probably attributable to the higher activity levels that season under the same occupancy condition. For instance, besides breakfast preparation and other cooking events, which happened on a daily basis for both seasons, 20 applesauce making events occurred during the summer campaign. Applesauce making events are clear indicators that the occupants were more active indoors in summer than in winter.

Compared with the effect of occupancy (including occupant activities), other factors only had modest impact on indoor FBAP levels. For example, the variable influence of outdoor FBAP during occupied conditions was only moderate. The contributions from outdoors were roughly estimated using geometric mean air-change rates across the campaign days, outdoor FBAP levels measured at the end of each campaign, and accounting for deposition. The contributions from outdoors were about  $7 \times 10^3 \text{ m}^{-3}$  and  $4 \times 10^3 \text{ m}^{-3}$  for the summer and winter campaign, respectively, considerably smaller than geometric mean values during awake and occupied conditions, which were in the range  $(16-36) \times 10^3 \text{ m}^{-3}$ .

(a)



(b)

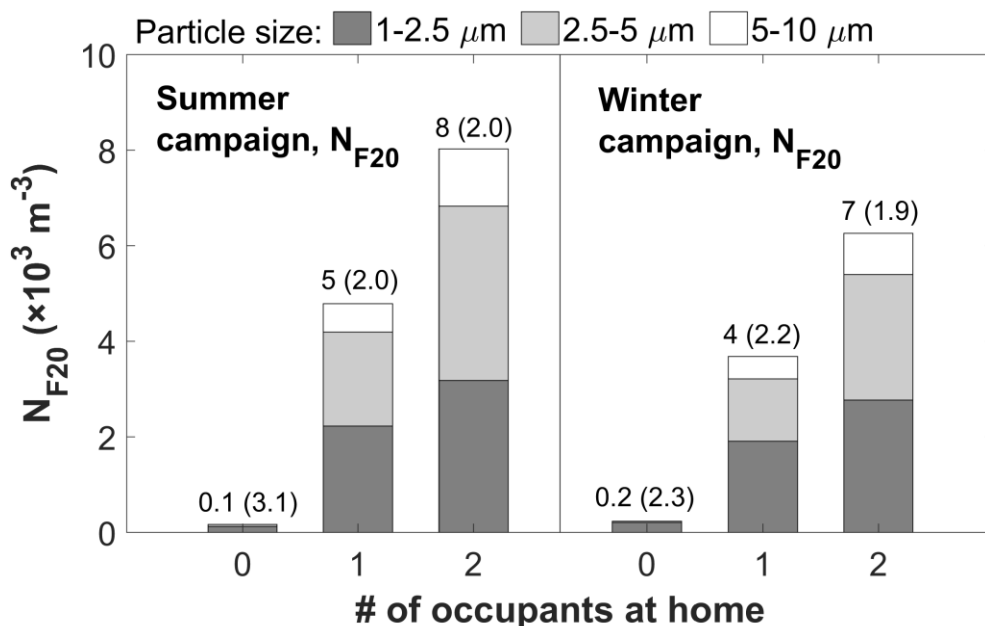


**Figure 2.** Geometric mean of hourly-averaged indoor (a) fluorescent ( $N_F$ ) and (b) highly fluorescent ( $N_{F20}$ ) particle concentrations associated with occupied conditions (vacant versus one or two occupants awake and at home), respectively. For the summer campaign, 39 hours were included for house vacant condition; 85 and 222 hours were included for house occupied with 1 and 2 occupants, respectively. For the winter campaign, 23 hours were included for house vacant condition; 90 and 137 hours were included for house occupied with 1 and 2 occupants, respectively. The GM (geometric standard deviation) values for size-integrated concentrations of  $N_F$  and  $N_{F20}$  (1-10  $\mu\text{m}$ ) are reported on top of the stacked bars. Periods when the occupants were asleep are excluded.

Particle size distributions of  $N_F$  and  $N_{F20}$  associated with occupancy levels and in outdoor air are presented in Figures S7 and S8, together with geometric means and geometric standard deviations of the best-fit lognormal distributions. As shown in Figure S7, when the house was vacant, about 90% of the FBAPs and highly fluorescent particles were in the 1-2.5  $\mu\text{m}$  size range, with a modeled mode at around 1.3  $\mu\text{m}$ . The main source of indoor FBAP and highly fluorescent particles during vacant periods was infiltration of outdoor materials. For occupied conditions, the modes of  $N_F$  and  $N_{F20}$  shifted to the larger diameters of 2.1  $\mu\text{m}$  and 3  $\mu\text{m}$ , respectively. The shifts were attributable to the presence of indoor emissions caused by human activities. FBAP and

highly fluorescent particle concentrations peaked in the 1-3  $\mu\text{m}$  range and 2-4  $\mu\text{m}$  range for occupied conditions, respectively. As displayed in Figure S8, the modeled modes of outdoor FBAPs were at about 3  $\mu\text{m}$ , in good agreement with previous studies.<sup>25,30</sup>

### 3.2 FBAP emissions for human activities

For the observational campaigns, 104 events were analyzed for the selected four activities including breakfast preparation, other cooking, making applesauce, and vacuuming. The number of FBAP particles emitted ( $F$ ) ranged from  $10^6$  to  $10^8$  particles per event. Figure 3 displays geometric mean emissions of fluorescent biological aerosol particles (FBAP,  $F$ ) and of highly fluorescent particles ( $F_{20}$ ) from various human activities. In central-tendency, the selected human activities emitted about  $14 \times 10^6$  to  $53 \times 10^6$  FBAP particles including  $2 \times 10^6$  to  $16 \times 10^6$  highly fluorescent particles per event. As can be seen in Figure 3, considerable portions of FBAP and highly fluorescent particles emitted were in the coarse size range (2-10  $\mu\text{m}$  diameter). (Numbers discussed in section 3.2 and section 3.3 are geometric mean (GSD) values unless otherwise specified.)

For food-related activities, such as breakfast preparation, other cooking, and applesauce making, potential sources of biological particles include direct shedding from the occupants, resuspension from clothing and flooring, biological particles aerosolized from tap water and boiling water (via bubble-bursting), and emissions from processing food.<sup>15,21,22,42,43</sup>

Breakfast preparation followed a relatively consistent pattern each day, as described in the SI, and resulted in similar FBAP emissions for the two campaigns. Although emissions during summer were slightly higher, the seasonal differences were not statistically significant for FBAP particles. For highly fluorescent particles, emissions during summer were significantly higher than during winter ( $p < 0.05$ , one-sided Mann-Whitney test). We speculate that the higher

$F_{20}$  might be attributable to enhanced shedding of bacteria-laden skin flakes as a result of reduced clothing coverage in summer.

Unlike breakfast preparation, other cooking events exhibited considerable day-to-day variability, likely attributable to more variable cooking styles for lunch and dinner preparation than for breakfast. Cooking during the summer campaign resulted in the highest FBAP emissions, which was approximately four times higher than cooking emissions during the winter campaign ( $p < 0.001$ , Student t-test). Similar trends were observed for highly fluorescent particles, although the difference was smaller than for FBAP. Summer cooking events resulted in approximately 2.3 times higher  $F_{20}$  than from winter cooking events ( $p = 0.01$ , one-sided Mann-Whitney test).

The seasonal difference in cooking emissions was further investigated by sorting cooking events into two major groups based on cooking style: fry/sauté (summer  $n = 10$ ; winter  $n = 10$ ); and boiling/steaming (summer  $n = 6$ ; winter  $n = 7$ ). For both groups, summer events showed significantly higher emissions than winter events ( $p < 0.05$ , one-sided Mann-Whitney test). The difference in fry/sauté events was mainly caused by one particular cooking activity, namely the making of ratatouille ( $n = 3$ ), which exhibited an average emission of  $630 \times 10^6$  FBAP particles, the highest among all events evaluated. (This cooking activity entailed pan-grilling vegetables on an electric range top at high heat, close to the smoking point of olive oil.) With ratatouille-making excluded, summer fry/sauté events still showed a higher median emission of  $27 \times 10^6$  FBAP particles compared to  $17 \times 10^6$  FBAP particles emitted from winter fry/sauté events; however, that difference is not statistically significant. For boiling/steaming events, the summer median emissions were  $48 \times 10^6$  FBAP particles, about four times higher than the winter median emissions of  $13 \times 10^6$  particles. Event durations were comparable between the two campaigns,

with some differences in ingredients used. Nevertheless, it is unclear if the seasonal difference in emissions is caused by differences in ingredients without additional information such as the amount of food prepared per event.

Applesauce making, which involved both occupants peeling and chopping apples harvested from the garden followed by stove-top cooking, caused the second highest FBAP emissions. Compared with breakfast preparation (summer), which was also undertaken by both occupants, applesauce making was associated with approximately 40% higher  $F$  but very similar  $F_{20}$ . We surmise that the sources of highly fluorescent particles are mainly human related rather than food related.

Some seasonal difference was observed at this house for surface microbial biomass. As reported by Adams et al.,<sup>44</sup> who sampled periodically wet surfaces (including the kitchen sink) in the studied house, greater biomass was detected in the summer campaign than during the winter campaign.

As shown in Figure 3, the FBAP emissions from vacuuming and wet mopping of the hard-surface flooring mostly ranged in size from 2 to 10  $\mu\text{m}$  with weak emission observed for the 1 to 2  $\mu\text{m}$  fraction. This pattern is different from previously reported total particle emissions, which were dominated by fine particles.<sup>23,45</sup> Potential sources of FBAP include biological particles emitted from the occupants (direct shedding and resuspension from clothing), emissions from vacuum bags and resuspended floor dust.

Manipulation experiments included showering and applying personal care products such as sunscreen and deodorant ( $t_s = 20$  min) and making a queen-size bed and folding previously worn clothes ( $t_s = 10$  min). As shown in Figure S9, size-resolved emissions from the showering events had a mode at 2.6  $\mu\text{m}$  for FBAPs and a mode at 4.4  $\mu\text{m}$  for highly fluorescent particles.

Figure S10 displays the particle size distributions of aerosolized shower water without anyone in the shower stall. Aerosolized shower water caused the  $N_F$  level to be elevated to approximately 4 times the background value, mainly in the diameter range 1-3  $\mu\text{m}$ , but no difference was observed for  $N_{F20}$  levels. This result suggests that shower water also contributed to FBAP emissions during the showering event, whereas highly fluorescent particle emissions were probably mainly attributable to emissions from the showering human subject. The size distribution of shower generated FBAPs compare well with findings from Bollin et al.<sup>46</sup>, who reported that about 90% of the *Legionella pneumophila*-laden particles emitted from shower heads were 1-5  $\mu\text{m}$  in diameter. Other than cooking during the summer campaign, showering caused the highest FBAP emissions in the 1-2  $\mu\text{m}$  range, likely attributable to FBAPs from aerosolized shower water. Regarding making the bed and folding clothes, size distributions of FBAP and highly fluorescent particle emissions had similar profiles, peaking in the 3-5  $\mu\text{m}$  diameter range, as shown in Figure S11. Potential sources of biological particles for bed making and clothes folding include direct shedding from the human subject plus the resuspension of bacteria-laden skin flakes and fungal spores from bedding and clothes.<sup>47,48</sup> Making bed and folding clothes together led to the highest FBAP and highly fluorescent particle emission in the 2-5  $\mu\text{m}$  and 5-10  $\mu\text{m}$  ranges, probably owing to resuspension from textiles. Humans shed 200-1000 million cells per day.<sup>49</sup> Bedding and clothing can act as a reservoir of skin flakes shed from humans and also of deposited airborne biological particles.

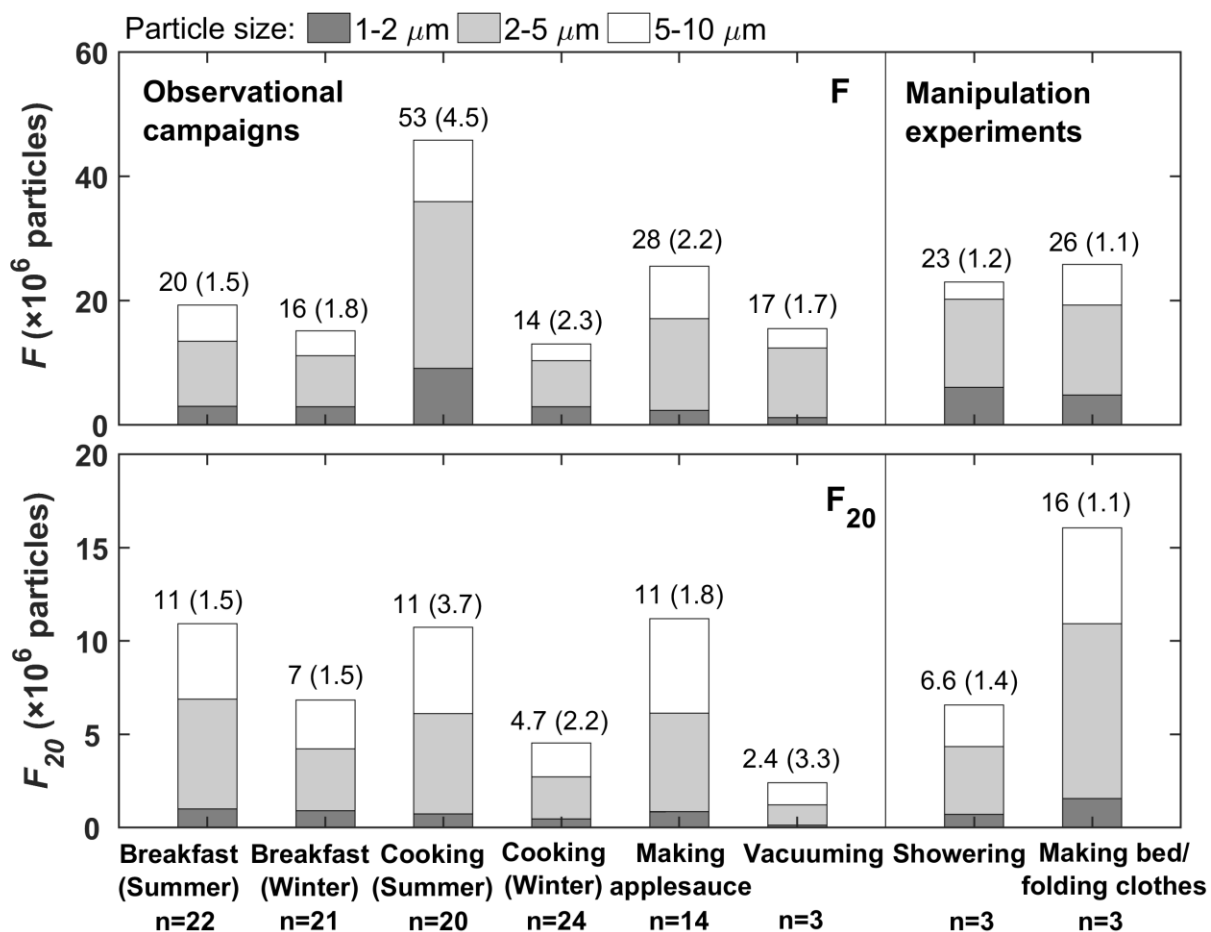


**Figure 3.** Geometric mean size-segregated emissions of FBAP particles ( $F$ ) (top panel) and (b) highly fluorescent particles ( $F_{20}$ ) (bottom panel) associated with selected human activities. The number of events analyzed is marked below each stacked bar. The GM (GSD) of size-integrated emissions (1-10  $\mu\text{m}$ ) are displayed on top of the stacked bars.

One source of uncertainty associated with estimating  $F$  is the lack of simultaneously measured outdoor FBAP concentrations. The contributions of outdoor FBAP were estimated using a single average outdoor level measured at the end of each campaign. Compared with indoor emissions, the estimated outdoor particle contributions represented a small fraction (GM < 15%) of the total  $N_F$  levels during emission events. Hence, the contribution to uncertainty because of a lack of detailed knowledge about outdoor levels is believed to be small. Another potential source of error is abiotic interference that could produce false positive FBAP counts. In

particular, it is feasible that the fry/sauté style of cooking could emit primary PAHs (e.g. from heated cooking oils) and cooking emissions might also contribute to secondary organic aerosol (SOA) formation.<sup>50,51</sup> Available evidence would suggest that these interferents are mainly found in submicron particles, with only a small probability of coagulating onto supermicron particles.<sup>31,52</sup> Evidence in this study regarding potential interferent contributions of PAH and SOA formation in relation to FBAP signals are not definitive, but do suggest that any interference was not a major contributor to the results. For instance, Figure S12 shows particle size distributions of ratatouille-making events, which, because of the high cooking temperature, were most likely to emit primary PAH. The size distribution of mean FBAP concentrations observed peaked at around 2-4  $\mu\text{m}$  instead of at the lower bound of the size spectrum, 1  $\mu\text{m}$ . In addition, the FBAP size distributions did not match total particle distributions, which peaked in the submicron size range. Similar trends were observed for other high-emitting cooking events. To our knowledge, the impact of cooking emissions on coarse FBAP counts has not been directly tested in any prior study.

### 3.3 Exposure assessment

Occupancy patterns for the two adults living in this house were sufficiently similar to justify grouping them for the purposes of statistical assessment of exposure. During the summer and winter campaigns, the occupants spent 10 hours per day (1.3) and 8.5 hours per day (1.5), respectively, awake and at home. Considering these awake and at home periods, the daily-averaged FBAP exposure concentration (1-10  $\mu\text{m}$ ) was  $40 \times 10^3 \text{ m}^{-3}$  (1.7) for summer and  $29 \times 10^3 \text{ m}^{-3}$  (1.3) for winter. Regarding highly fluorescent particles, the daily-averaged exposure concentration was  $9 \times 10^3 \text{ m}^{-3}$  (1.5) for summer and  $7 \times 10^3 \text{ m}^{-3}$  (1.3) for winter. Figure 4 displays the cumulative distribution of daily-integrated FBAP and highly fluorescent particle



exposures determined during the summer and winter campaigns, respectively. In general, at-home occupant exposures were higher for the summer campaign, owing to the combined effects of higher occupancy level and enhanced exposure concentrations.

Differences were estimated between exposure concentrations assessed using time-resolved concentrations during awake periods of occupancy and the more conventional approaches, either employing time-integrated concentrations (several hours or longer) or snapshot concentrations (several minutes or shorter). An averaging time of 24 h was chosen to compute time-integrated FBAP concentrations using data collected in both campaigns. As shown in Figure S13, using 24-h average, including non-occupied periods, FBAP daily exposure concentrations would be underestimated by approximately 33% in the studied residence. This finding is in good agreement with a previous study evaluating  $PM_{2.5}$  exposure in indoor environments.<sup>53</sup> Regarding snapshot concentrations, it is a challenge for such an approach to obtain representative samples for exposure assessment owing to the rapidly changing indoor FBAP levels associated with time-varying occupancy and occupant activities. As illustrated in Figure 2, samples taken during unoccupied periods may underestimate exposure concentrations by an order of magnitude. In addition, when assessing exposure in a given microenvironment, only the concentrations measured when the receptor is present in the given microenvironment are relevant. During occupancy periods, indoor FBAP concentrations can vary as much as two orders of magnitude within a day. Figure S4 shows exposure time profiles for a typical day as an example. Moreover, a measurement team must take great care so that their biological particle emissions during setup and sampling periods do not confound sampling results; that risk is particularly large for the snapshot style of indoor bioaerosol measurement.

Because of source proximity and the personal cloud effect, FBAP concentrations as measured here with a stationary monitor might be lower than the actual exposure concentrations.<sup>54</sup> In addition, contributions to exposure that occurred during sleeping hours were not evaluated in this study. Consequently, the presented FBAP exposures represent lower bounds of daily residential bioaerosol exposure at site H1 for subjects M1 and F1.

As discussed in the previous section, abiotic interferents might have led to some overestimation of FBAP concentrations during cooking events. If cooking events were excluded from the analysis, geometric mean daily-integrated exposure would have been reduced by an average of 13% and 11% for the summer and winter campaigns, respectively.

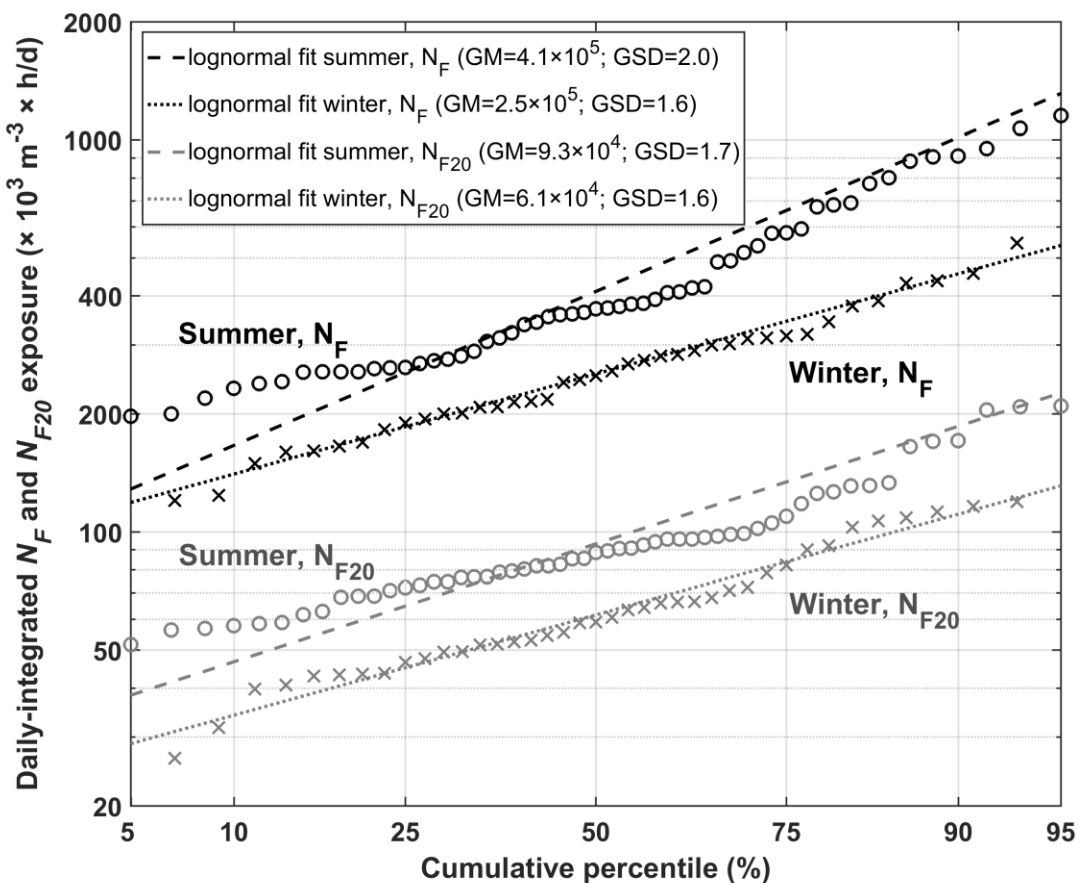


**Figure 4.** Daily-integrated occupant exposures ( $\times 10^3 \text{ m}^{-3} \times \text{h/d}$ ) to FBAPs,  $N_F$  (black), and highly fluorescent particles,  $N_{F20}$  (gray) during the summer (circles) and winter campaigns

(crosses). Best-fit lognormal distributions are plotted, with modeled geometric means and geometric standard deviations reported in the legend. Exposures for the two subjects were not statistically different, so they are combined and presented without differentiation in this plot.

#### 4 Conclusion

Knowledge developed in this study can contribute to a better understanding of bioaerosol concentrations, emissions, and human exposure in residential environments. First, human occupancy and activities were seen to be important sources of FBAPs even in a moderately large home with only two occupants. Human occupancy enhanced indoor FBAP and highly fluorescent particle concentrations by an order of magnitude above the levels observed during unoccupied periods. Elevated FBAP and highly fluorescent particle concentrations were associated with increased occupancy level. For occupied conditions, the modes of  $N_F$  and  $N_{F20}$  were found to be in the 1-3  $\mu\text{m}$  and 2-4  $\mu\text{m}$  particle size ranges, respectively. Second, common household activities, such as cooking, vacuuming, showering, and making a bed, can substantially emit indoor FBAPs. This finding suggests a possibility that mitigating emissions from these activities, for example through laundering bedding material more frequently to minimize biological particle accumulation, might lead to a reduction of bioaerosol exposure and associated detrimental health outcomes, such as allergic asthma. In central tendency, selected human activities emitted  $14 \times 10^6$  to  $53 \times 10^6$  FBAP particles including  $2 \times 10^6$  to  $16 \times 10^6$  highly fluorescent particles per event. The results can be used in indoor air quality models to estimate the impact of human activities on indoor FBAP levels. Compared with indoor sources, estimated outdoor contributions to indoor FBAP levels were no more than moderate. Third, to assess FBAP exposure in residences, only concentrations measured during occupancy periods should be used, due to the strong influences of occupancy level and occupant activities. Including concentrations measured during unoccupied periods in exposure assessment would

likely underestimate human exposure to FBAPs to a substantial extent. Considering only awake and at-home periods, the geometric mean daily-integrated FBAP exposures (1-10  $\mu\text{m}$ ) were estimated to be  $410 \times 10^3 \text{ m}^{-3} \times \text{h/d}$  for summer (2.0) and  $250 \times 10^3 \text{ m}^{-3} \times \text{h/d}$  (1.6) for winter.

In this work, only a single house was studied. Clearly bioaerosol concentrations and emissions measured in one house cannot represent general conditions. The seasonal difference observed in this study might not apply to other parts of the country. However, the type of deep probing undertaken here does elucidate important mechanisms and processes, contributing to a foundation of knowledge that supports the design and interpretation of studies that would sample more broadly. Future work could be undertaken using similar methods as employed here to study the influence of different household characteristics on indoor bioaerosol levels. Factors to consider include the role of central heating and air-conditioning systems, (including filter characteristics), efficacy of portable air cleaning devices, and the effects of occupant density, flooring materials, and pet presence. Although the estimated influence of outdoor levels on indoor FBAP concentration was only moderate in this work, future studies would usefully include simultaneous measurement of indoor and outdoor concentrations if biological particles of outdoor origin are of interest. Also, more research is needed to better understand the possible contributions of indoor interferents to FBAP signals and, if significant, to assess how best to discriminate between fluorescent biological particles and abiotic interferents.

## Acknowledgements

**This work was supported by research grants from the Alfred P. Sloan Foundation (Chemistry of Indoor Environments and Microbiology of the Built Environment). The authors deeply appreciate the occupants for volunteering their house and facilitating monitoring. We thank Rachel Adams, Despoina Lympelopoulou, and other members of the Berkeley BIMERC team for their valuable input.**

## References

1. Kulkarni P, Baron PA, Willeke K, Eds. *Aerosol Measurement: Principles, Techniques, and Applications*, 3<sup>rd</sup> edition, Hoboken, NJ: John Wiley & Sons; 2011.
2. Yang W, Elankumaran S, Marr LC. Concentrations and size distributions of airborne influenza A viruses measured indoors at a health centre, a day-care centre and on aeroplanes, *J R Soc Interface*. 2011;8:1176–1184.
3. Qian J, Hospodsky D, Yamamoto N, Nazaroff WW, Peccia J. Size-resolved emission rates of airborne bacteria and fungi in an occupied classroom. *Indoor Air*. 2012;22:339–351.
4. Eduard W. Fungal spores: A critical review of the toxicological and epidemiological evidence as a basis for occupational exposure limit setting. *Crit Rev Toxicol*. 2009;39:799–864.
5. Górny RL, Dutkiewicz J, Krysinska-Traczyk E. Size distribution of bacterial and fungal bioaerosols in indoor air. *Ann Agric Environ Med*. 1999;6:105–113.
6. Hyvärinen A, Vahteristo M, Meklin T, Jantunen M, Nevalainen A, Moschandreas D. Temporal and spatial variation of fungal concentrations in indoor air. *Aerosol Sci Technol*. 2001;35:688–695.
7. Reponen T, Hyvärinen A, Ruuskanen J, Raunemaa T, Nevalainen A. Comparison of concentrations and size distributions of fungal spores in buildings with and without mould problems. *J Aerosol Sci*. 1994;25:1595–1603.
8. Burge H. Bioaerosols: Prevalence and health effects in the indoor environment. *J Allergy Clin Immunol*. 1990;86:687–701.

9. Edwards MR, Bartlett NW, Hussell T, Openshaw P, Johnston SL. The microbiology of asthma. *Nature Rev Microbio*. 2012;10:459–471.
10. Górny RL, Dutkiewicz J. Bacterial and fungal aerosols in indoor environment in central and eastern European countries. *Ann Agric Environ Med*. 2002;9:17–23.
11. Jo WK, Seo YJ. Indoor and outdoor bioaerosol levels at recreation facilities, elementary schools, and homes. *Chemosphere*. 2005;61:1570–1579.
12. Mentşe S, Arisoy M, Rad AY, Güllü G. Bacteria and fungi levels in various indoor and outdoor environments in Ankara, Turkey. *Clean – Soil Air Water*. 2009;37:487–493.
13. Klepeis NE, Nelson WC, Ott WR, et al. The National Human Activity Pattern Survey (NHAPS): a resource for assessing exposure to environmental pollutants. *J Expo Anal Environ Epidemiol*. 2001;11:231–252.
14. Bhangar S, Huffman JA, Nazaroff WW. Size-resolved fluorescent biological aerosol particle concentrations and occupant emissions in a university classroom, *Indoor Air*. 2014;24:604–617.
15. Bhangar S, Adams RI, Pasut W, et al. Chamber bioaerosol study: human emissions of size-resolved fluorescent biological aerosol particles. *Indoor Air*. 2016;26:193–206.
16. Chen Q, Hildemann LM. The effects of human activities on exposure to particulate matter and bioaerosols in residential homes. *Environ Sci Technol*. 2009;43:4641–4646.
17. Toivola M, Alm S, Reponen T, Kolari S, Nevalainen A. Personal exposures and microenvironmental concentrations of particles and bioaerosols. *J Environ Monit*. 2002;4:166–174.
18. Bollin GE, Plouffe JF, Para MF, Hackman B. Aerosol containing *Legionella pneumophila* generated by shower heads and hot-water faucets. *Appl Environ Microbiol*. 1985;50:1128–1131.
19. Duguid JP. The size and the duration of air-carriage of respiratory droplets and droplet-nuclei. *J Hyg*. 1946;44:471–479.
20. Goebes MD, Boehm AB, Hildemann LM. Contributions of foot traffic and outdoor concentrations to indoor airborne *Aspergillus*. *Aerosol Sci Technol*. 2011;45:352–363.
21. Hospodsky D, Qian J, Nazaroff WW, et al. Human occupancy as a source of indoor airborne bacteria. *PLoS One*. 2012;7:e34867.

22. Jürgensen CW, Madsen AM. Influence of everyday activities and presence of people in common indoor environments on exposure to airborne fungi. *AIMS Environ Sci.* 2016;3:77–95.
23. Knibbs LD, He C, Duchaine C, Morawska L. Vacuum cleaner emissions as a source of indoor exposure to airborne particles and bacteria. *Environ Sci Technol.* 2012;46:534–542.
24. Lee JH, Jo WK. Characteristics of indoor and outdoor bioaerosols at Korean high-rise apartment buildings. *Environ Res.* 2006;101:11–17.
25. Huffman JA, Treutlein B, Pöschl U. Fluorescent biological aerosol particle concentrations and size distributions measured with an Ultraviolet Aerodynamic Particle Sizer (UV-APS) in Central Europe. *Atmos Chem Phys.* 2010;10:3215–3233.
26. Liu Y, Misztal PK, Xiong J, et al. Detailed investigation of ventilation rates and airflow patterns in a northern California residence. *Indoor Air.* (revised submission 20 February 2018).
27. Eng J, Lynch RM, Balaban RS. Nicotinamide adenine dinucleotide fluorescence spectroscopy and imaging of isolated cardiac myocytes. *Biophys J.* 1989;55:621–630.
28. Hairston PP, Ho J, Quant FR. Design of an instrument for real-time detection of bioaerosols using simultaneous measurement of particle aerodynamic size and intrinsic fluorescence. *J Aerosol Sci.* 1997;28:471–482.
29. Li JK, Asali EC, Humphrey AE, Horvath JJ. Monitoring cell concentration and activity by multiple excitation fluorometry. *Biotechnol Prog.* 1991;7:21–27.
30. Healy DA, Huffman JA, O'Connor DJ, Pöhlker C, Pöschl U, Sodeau JR. Ambient measurements of biological aerosol particles near Killarney, Ireland: a comparison between real-time fluorescence and microscopy techniques. *Atmos Chem Phys.* 2014;14:8055–8069.
31. Huffman JA, Sinha B, Garland RM, et al. Size distributions and temporal variations of biological aerosol particles in the Amazon rainforest characterized by microscopy and real-time UV-APS fluorescence techniques during AMAZE-08. *Atmos Chem Phys.* 2012;12:11997–12019.
32. Pöschl U, Martin ST, Sinha B, et al. Rainforest aerosols as biogenic nuclei of clouds and precipitation in the Amazon. *Science.* 2010;329:1513–1516.

33. Schumacher CJ, Pöhlker C, Aalto P, et al. Seasonal cycles of fluorescent biological aerosol particles in boreal and semi-arid forests of Finland and Colorado. *Atmos Chem Phys*. 2013;13:11987–12001.
34. Pereira ML, Knibbs LD, He C, et al. (2017). Sources and dynamics of fluorescent particles in hospitals. *Indoor Air*. DOI: 10.1111/ina.12380.
35. Bones DL, Henricksen DK, Mang SA, et al. Appearance of strong absorbers and fluorophores in limonene-O<sub>3</sub> secondary organic aerosol due to NH<sub>4</sub><sup>+</sup>-mediated chemical aging over long time scales. *J Geophys Res*. 2010;115:D05203.
36. Lee HJ, Laskin A, Laskin J, Nizkorodov SA. Excitation-emission spectra and fluorescence quantum yields for fresh and aged biogenic secondary organic aerosols. *Environ Sci Technol*. 2013;47:5763–5770.
37. Pöhlker C, Huffman JA, Pöschl U. Autofluorescence of atmospheric bioaerosols – fluorescent biomolecules and potential interferences. *Atmos Meas Tech*. 2012;5:37–71.
38. Savage NJ, Krentz CE, Könemann T, et al. Systematic characterization and fluorescence threshold strategies for the wideband integrated bioaerosol sensor (WIBS) using size-resolved biological and interfering particles. *Atmos Meas Tech*. 2017;10:4279–4302.
39. Agranovski V, Ristovski ZD, Ayoko GA, Morawska L. Performance evaluation of the UVAPS in measuring biological aerosols: Fluorescence spectra from NAD(P)H coenzymes and riboflavin. *Aerosol Sci Technol*. 2004;38:354–364.
40. Thatcher TL, Lai AC, Moreno-Jackson R, Sextro RG, Nazaroff WW. Effects of room furnishings and air speed on particle deposition rates indoors. *Atmos Environ*. 2002; 36:1811–1819.
41. Heo KJ, Lim CE, Kim HB, Lee BU. Effects of human activities on concentrations of culturable bioaerosols in indoor air environments. *J Aerosol Sci*. 2017;104:58–65.
42. Prussin II AJ, Schwake DO, Marr LC. Ten questions concerning the aerosolization and transmission of *Legionella* in the built environment. *Build Environ*. 2017;123:684–695.
43. Blanchard DC, Syzdek LD. Water-to-air transfer and enrichment of bacteria in drops from bursting bubbles. *Appl Environ Microbiol*. 1982;43:1001–1005.
44. Adams RI, Lympelopoulou DS, Misztal PK, et al. Microbes and associated soluble and volatile chemicals on periodically wet household surfaces. *Microbiome*. 2017;5:128.



45. Ferro AR, Kopperud RJ, Hildemann LM. Source strengths for indoor human activities that resuspend particulate matter. *Environ Sci Technol*. 2004;38:1759–1764.
46. Bollin GE, Plouffe JF, Para MF, Hackman B. Aerosols containing *Legionella pneumophila* generated by shower heads and hot-water faucets. *Appl Environ Microbiol*. 1985;50:1128–1131.
47. Davies RR, Noble WC. Dispersal of bacteria on desquamated skin. *Lancet*. 1962;280:1295–1297.
48. Lehtonen M, Reponen T, Nevalainen A. Everyday activities and variation of fungal spore concentrations in indoor air. *Int Biodeter Biodegr*. 1993;31:25–39.
49. Milstone LM. Epidermal desquamation. *J Derm Sci*. 2004;36:131–140.
50. Klein F, Farren NJ, Bozzetti C, et al. Indoor terpene emissions from cooking with herbs and pepper and their secondary organic aerosol production potential. *Sci Rep*. 2016;6:36623.
51. Liu T, Li Z, Chan M, Chan CK. Formation of secondary organic aerosols from gas-phase emissions of heated cooking oils. *Atmos Chem Phys*. 2017;17:7333–7344.
52. Jimenez JL, Canagaratna MR, Donahue NM, et al. Evolution of organic aerosols in the atmosphere. *Science*. 2009;326:1525–1529.
53. Wierzbicka A, Bohgard M, Pagels JH, et al. Quantification of differences between occupancy and total monitoring periods for better assessment of exposure to particles in indoor environments. *Atmos Environ*. 2015;106:419–428.
54. Licina D, Tian Y, Nazaroff WW. Emission rates and the personal cloud effect associated with particle release from the perihuman environment. *Indoor Air*. 2017;27:791–802.